

Phase transitions induced by solid solution in stuffed derivatives of quartz: A powder synchrotron XRD study of the $\text{LiAlSiO}_4\text{-SiO}_2$ join

HONGWU XU^{1,*}, PETER J. HEANEY², AND GEORGE H. BEALL³

¹Department of Geosciences and Princeton Materials Institute, Princeton University, Princeton, New Jersey 08544, U.S.A.

²Department of Geosciences, Pennsylvania State University, University Park, Pennsylvania 16802, U.S.A.

³Corning Incorporated, Sullivan Park FR-51, Corning, New York 14831, U.S.A.

ABSTRACT

The crystal structures of stuffed derivatives of quartz within the $\text{Li}_{1-x}\text{Al}_{1-x}\text{Si}_{1+x}\text{O}_4$ system have been refined by Rietveld analysis of powder synchrotron X-ray diffraction (XRD) data. Our results reveal an Al-Si order-disorder transition at $x \sim 0.3$ and a β - α displacive transformation at $x \sim 0.65$. Structural variations across the series result from an interplay of three mechanisms: tetrahedral tilting associated with Al-Si order-disorder; Li positional disorder along structural channels parallel to *c*; and tetrahedral rotation related to the β - α transition. At both microscopic (local bonding) and macroscopic (spontaneous strain) scales, the substitution of Li^+ and Al^{3+} for Si^{4+} closely mimics temperature in its effect on the quartz framework.

INTRODUCTION

The substitution of impurity cations into normally vacant cavities or tunnels in crystal structures can induce systematic changes in framework geometry, and these topological modifications as well as electrostatic interactions may alter the transition behavior of the mineral. Typically (but not always), such interstitial cations prop open network cages and stabilize higher-temperature polymorphs. In quartz, this effect was documented by Keith and Tuttle (1952), who found that substitution of 5200 ppm $\text{M}^+ + \text{Al}^{3+}$ for Si^{4+} ($\text{M}^+ = \text{Li}^+, \text{Na}^+, \text{K}^+, \text{and H}^+$) lowered the β -to- α inversion by 36 K. Subsequent studies by Ghiorsio et al. (1979) and by Smith and Steele (1984) confirmed these trends and demonstrated a roughly linear relationship between Al concentration and the critical temperature. Because the natural samples examined in these investigations contained a variety of impurities, however, correlations of T_c with dopant contents exhibited a large degree of scatter.

Salje et al. (1991) used Landau analysis to develop a quantitative model to gauge the effects of impurity substitutions on phase transitions, and they observed that when impurity concentrations N are high ($\gg 10^{23}/\text{cm}^3$), the renormalized critical temperature, T_c^* , should vary linearly with T_c , i.e., $T_c^* = T_c - \xi N$, where ξ is a constant. One implication of this model is that impurities may act as a proxy for temperature, such that variations in dopant concentration at constant temperature may induce a structural transition sequence that is nearly identical to that produced by heating or cooling of the pure end-member.

Quantifying this interplay between impurities and critical temperatures is especially important in mineral systems, where crystals are rarely compositionally pure. Nevertheless, surpris-

ingly few studies of silicate systems (e.g., McGuinn and Redfern 1994) have included high-resolution comparisons of the structural effects of doping with transitional modifications induced by temperature. In this work, we examined seven compositions along the β -eucryptite (LiAlSiO_4)— α -quartz (SiO_2) join to characterize the framework expansion induced by the substitution $\text{Li}^+ + \text{Al}^{3+} \rightarrow \text{Si}^{4+}$ within quartz at room temperature. Our Rietveld analyses of powder synchrotron XRD data revealed evidence for two structural transformations across the series. A Landau-style analysis of the impurity-driven transition between α and β quartz-type modifications is consistent with the model for the α - β transformation induced by temperature in pure quartz (Carpenter et al. 1998a).

BACKGROUND

The structure of β -quartz consists of parallel threefold and sixfold helices of silica tetrahedra that produce open channels parallel to *c*. Upon cooling, this structure transforms displacively to the denser α -quartz configuration at 846 K, involving a space group change from $P6_222$ or $P6_422$ to $P3_221$ or $P3_121$ (reviewed in Heaney 1994). While pure β -quartz is not quenchable, the incorporation of small cations (such as Li^+ and Zn^{2+}) into the structural channels can prop open the framework and stabilize the β -quartz structure at room temperature (Palmer 1994; Beall 1994; Müller 1995 and references therein). Charge balance can be achieved by replacing a fraction of the Si^{4+} with cations having lower valences, such as Al^{3+} and B^{3+} . The resulting phases are classified as “stuffed derivatives of β -quartz” (Buerger 1954).

The stabilization of the β -quartz structure at room temperature, however, can only be achieved when the concentration of the substitutional cations exceeds a critical threshold. When dopant concentrations fall below this threshold, the silica framework will adopt the denser α -quartz modification because the impurity cation content is too low to sustain the more expanded β -quartz framework (Petzoldt 1967; Beall 1994).

*Present address: Thermochemistry Facility, Department of Chemical Engineering and Materials Science, University of California at Davis, Davis, California 95616, U.S.A. E-mail: hxu@ucdavis.edu

Stuffed derivatives of quartz with the composition $\text{Li}_{1-x}\text{Al}_{1-x}\text{Si}_{1+x}\text{O}_4$, $0 \leq x < 1$, belong to the so-called LAS ($\text{Li}_2\text{O}-\text{Al}_2\text{O}_3-\text{SiO}_2$) system (Beall 1994), and compounds having the β -quartz structure ($0 \leq x < \sim 0.67$) (Nakagawa and Izumitani 1972) constitute one of the major families of materials that exhibit low coefficients of thermal expansion (Roy 1995). For example, the end-member β -eucryptite has long been known to maintain a nearly constant volume from room temperature to 1473 K (Schulz 1974). Our recent synchrotron X-ray and neutron diffraction studies of β -eucryptite demonstrated that near-zero thermal expansion persists to temperatures as low as 20 K (Lichtenstein et al. 1998; Xu et al. 1999a). Therefore, these materials can serve not only in high-temperature applications (such as domestic cookware and jet engine components), but they are suitable as cryogenic glass-ceramics as well.

Although the interest in these materials has largely derived from their unique thermal properties, investigations of the LiAlSiO_4 - SiO_2 system can facilitate the understanding of general crystal-chemical systematics associated with the charge-coupled substitution M^+ (or $1/2 \text{M}^{2+}$) + $\text{Al}^{3+} \rightarrow \text{Si}^{4+}$, or $\text{M}^{2+} + \text{Al}^{3+} \rightarrow \text{M}^+ + \text{Si}^{4+}$ (where M is an alkaline or alkaline-earth cation or H^+). Because Si^{4+} and Al^{3+} are the two most abundant cations in the Earth's crust, these types of substitutions occur in many mineral groups, such as feldspars and zeolites. In these minerals, they can induce Al-Si order-disorder and other structural phase transitions. However, the complex subsolidus reactions in many systems, especially feldspars (e.g., Ribbe 1983), make it very difficult to isolate the effects that a single transition, particularly Al-Si order-disorder, exerts on crystal chemistry. By contrast, stuffed derivatives of quartz along the LiAlSiO_4 - SiO_2 join are relatively simple in structure, and thus they offer a better solid-solution series for studying Al-Si ordering (Xu et al. 1999b; Phillips et al. 2000). In addition, the quartz-eucryptite system allows a direct comparison of the α - β quartz-like transition induced by the substitution of $\text{Li}^+ + \text{Al}^{3+}$ for Si^{4+} with the temperature-driven α - β transformation. Since this transition is one of the most exhaustively studied displacive transitions (see reviews by Heaney and Veblen 1991; Heaney 1994; Dolino and Vallade 1994; Dorogokupets 1995), such a study may provide insights into the general ways in which impurities affect phase transitions.

EXPERIMENTAL METHODS

Sample synthesis

Stuffed quartz-derivative phases with the composition $\text{Li}_{1-x}\text{Al}_{1-x}\text{Si}_{1+x}\text{O}_4$, with $x = 0, 0.2, 0.33, 0.5, 0.69, 0.7$, and 0.9 , were prepared in this study. Because these phases exhibit different regions of thermodynamic stability and metastability, three synthesis methods were employed: (1) high-temperature sintering for $x = 0$ and 0.2 ; (2) high-pressure, high-temperature processing for $x = 0.33, 0.5, 0.7$ and 0.9 ; and (3) glass annealing for $x = 0.69$. Detailed synthesis and sample characterization procedures have been described in Xu et al. (1999b).

XRD data collection

Powder XRD measurements were carried out with a linear position-sensitive detector (PSD) at beam line X7A (Cox et al.

1988) of the National Synchrotron Light Source (NSLS), Brookhaven National Laboratory (BNL). The wavelengths used ranged from 0.7 to 0.8 Å, as calibrated using a CeO_2 standard. The powder samples were sealed in silica-glass capillaries of 0.2 mm-diameter and, to minimize preferred orientation, the capillaries were either fully rotated or rocked through $\pm 10^\circ$ during each data collection. Data were collected from 7 to 55° 2θ in step-scan mode using steps of 0.25° with counting times of 10 s (7 – 15°), 20 s (15 – 30°), 40 s (30 – 45°), and 80 s (45 – 55°) per step.

Structure refinements

Rietveld refinements for the $\text{Li}_{1-x}\text{Al}_{1-x}\text{Si}_{1+x}\text{O}_4$ compounds were performed using the General Structure Analysis System (GSAS) program of Larson and Von Dreele (1994). Depending on the composition (and thus the structure), the starting atomic parameters are taken from the following sources: for $x = 0$ and 0.2 , the study of β -eucryptite by Guth and Heger (1979); for $x = 0.33$ and 0.5 , the study of $\text{Li}_{0.67}\text{Al}_{0.67}\text{Si}_{1.33}\text{O}_4$ by Li (1968); and for $x = 0.69, 0.7$, and 0.9 , the study of α -quartz by Will et al. (1988).

We note that our refinements for the derivatives of α -quartz ($x = 0.69, 0.7$, and 0.9) are based on a unit-cell whose setting is consistent with the *International Tables for Crystallography* (Hahn 1996) but different from that used in many other diffraction studies of α -quartz. Crystallographers commonly eschewed the standard setting for space groups $P3_221$ and $P3_121$ because the standard origin is displaced by $c/3$ relative to that for the supergroups $P6_222$ and $P6_122$; this discrepancy obscures the close relationship between the structures of α - and β -quartz (O'Keeffe and Hyde 1996). As discussed in Heaney (1994), proper crystallographic usage dictates that we report atomic coordinates referenced to the standard origin of the *International Tables of Crystallography*. These coordinates are fully consistent with GSAS and most other refinement and plotting programs.

All of our refinements followed the same sequence: after scale factor and four RDF (radial distribution function, needed for modeling the background from the glass capillary) background terms for each histogram had converged, specimen displacement and lattice parameters were added and optimized. Between two and ten additional background terms were then added for each histogram, and the peak profiles were fitted to symmetric pseudo-Voigt functions with a peak asymmetry correction (Thompson et al. 1987; Finger et al. 1994). Upon convergence of the above parameters, atomic positions and isotropic temperature factors for Li, Al, Si, and O were refined.

RESULTS AND DISCUSSION

Sample purity

Although the diffraction patterns produced by most of our samples indicated single phases consistent with their nominal compositions, the diffraction peaks for samples with $x = 0.5$ and 0.9 exhibited shoulders suggestive of two intergrown phases with slightly different lattice constants (Fig. 1; Table 1). As a result, our refinements for these two compositions were based on two-component phases. It is not clear, however, whether

the biphasic mixtures are due to incomplete reaction during high-pressure synthesis or whether they reflect equilibrium immiscibility at the annealing temperatures and pressures. Nevertheless, as the differences between the cell parameters of the coexisting phases are small, so that their compositional differences probably also are small, we treated them as single phases for analyzing the variation in cell dimensions across the series. Thus, weighted average lattice constants were calculated based on molar ratios of two intergrown phases (Table 1). For another high-pressure product with $x = 0.7$, diffraction peaks exhibited even more complex splittings suggestive of five coexisting phases, and we were unable to determine their

individual cell dimensions by Rietveld analysis. Instead, a glass-annealed sample with a similar composition ($x = 0.69$) was studied.

Cation disordering and symmetry change

Previous structure analyses of the end-member β -eucryptite have revealed that its Al and Si atoms are ordered within alternate layers normal to c (Winkler 1948; Buerger 1954; Tscherry and Laves 1970; Schulz and Tscherry 1972a, 1972b; Tscherry et al. 1972a, 1972b; Pillars and Peacor 1973; Xu et al. 1999a, 1999c). The Al-Si order produces superlattice reflections with $h, k = \text{even}; l = \text{odd}$ (such as 201 and 003), which are characteristic of the β -eucryptite structure (Fig. 2a). However, with increasing silica content, the superlattice reflections become weaker and no longer can be discerned for phases with $x \geq 0.33$ (Fig. 2b), suggesting a loss of long-range Al-Si order for these compositions. Therefore, in our refinements, we used the β -eucryptite structure (space group $P6_222$) (Guth and Heger 1979) as the starting model for $0 \leq x < 0.33$ and the β -quartz stuffed-derivative structure $\text{Li}_{0.67}\text{Al}_{0.67}\text{Si}_{1.33}\text{O}_4$ (space group $P6_222$) (Li 1968) for $x \geq 0.33$.

Refinements based on the structure model of Li (1968), however, yielded poor goodnesses of fit when $x \geq 0.69$ (e.g., $\chi^2 = 4.29$ for $x = 0.5$ but $\chi^2 = 10.43$ for $x = 0.69$). We noticed that this discrepancy could be attributed to differences in the relative intensities of some reflections for the two compositional ranges. As shown in Figure 3, for example, the 111 peak is evident in the diffraction pattern of the 0.69 phase, whereas it is not discernible for $x = 0.33$. This means that the true structure for $x \geq 0.69$ is not strictly β -quartz-like. Hence, we tried to refine the structures for the compositional range $0.69 \leq x < 1$ in the space group of α -quartz, $P3_221$ (Will et al. 1988), and the χ^2 improved significantly (e.g., from 10.43 to 4.06 for the 0.69 phase).

Our final refined lattice parameters, atomic positions, temperature factors, T-O ($T = \text{Si, Al}$) bond lengths, and agreement indices for the refinements are presented in Tables 1–5.

Unit-cell parameters and structural transformations

The unit-cell parameters of the ordered structure (a_o, c_o, V_o) are related to those of the disordered phase (a_d, c_d, V_d) by $a_o = 2 a_d, c_o = 2 c_d$, and $V_o = 8 V_d$ (Figs. 4a–4f). Figures 5a–5c show the dependence of unit-cell dimensions on Si substitution for Li+Al in terms of the disordered cell; the cell param-

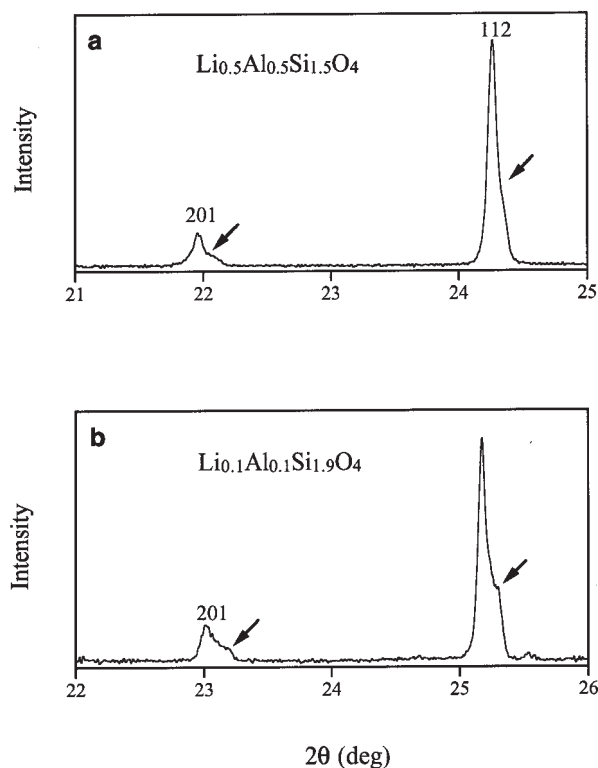


FIGURE 1. Peak splitting of the $\text{Li}_{1-x}\text{Al}_{1-x}\text{Si}_{1+x}\text{O}_4$ samples with $x = 0.5$ and 0.9 reveals the intergrowth of two phases.

TABLE 1. Unit-cell dimensions and refinement parameters of the stuffed-quartz phases $\text{Li}_{1-x}\text{Al}_{1-x}\text{Si}_{1+x}\text{O}_4$

x	a (Å)	c (Å)	V (Å ³)	R_{wp} (%)	R_p (%)
0*	10.49710(5)	11.19513(7)	1068.282(9)	5.51	3.83
0.2	10.4949(2)	10.9650(3)	1045.88(6)	6.70	5.23
0.33	5.2102(1)	5.4551(1)	128.242(4)	6.74	4.95
0.5 A	5.1651(1)	5.4571(1)	126.082(7)		
B	5.1384(4)	5.4589(3)	124.821(13)		
avg†	5.1609(1)	5.4574(1)	125.880(6)	4.50	3.72
0.69	5.0865(1)	5.4451(1)	122.004(4)	4.75	3.95
0.9 A	4.9672(2)	5.4187(1)	115.783(8)		
B	4.9380(3)	5.4123(3)	114.292(11)		
avg†	4.9567(2)	5.4164(1)	115.246(6)	6.77	5.94
1‡	4.91239(4)	5.40385(7)	112.933		

* From Xu et al. (1999a).

† Calculated based on molar ratio (A/B) of the two phases: 84/16 for $x = 0.5$ and 64/36 for $x = 0.9$.

‡ From Will et al. (1988).

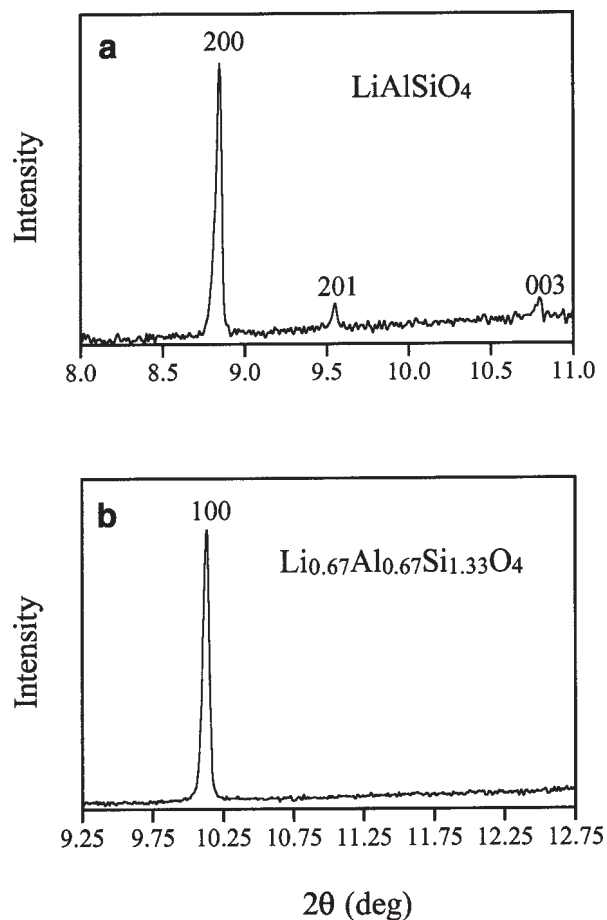


FIGURE 2. Synchrotron XRD patterns for the $\text{Li}_{1-x}\text{Al}_x\text{Si}_{1+x}\text{O}_4$ phases with (a) $x = 0$ and (b) $x = 0.33$. Note the superlattice peaks 201 and 003 are present in pattern (a) but absent in (b). Pattern (a) is indexed in terms of the ordered cell (a_o, c_o), whereas pattern (b) is based on the disordered quartz-like cell (a_d, c_d), where $a_o = 2a_d$; $c_o = 2c_d$.

TABLE 2. Atomic coordinates and isotropic temperature factors of ordered β -eucryptite (LiAlSiO_4) (space group $F\bar{6}_222$)*

Atom	x	y	z	U (\AA^2)†
Li1	0	0	0.5	0.0200(5)
Li2	0.5	0	0	0.0200(5)
Li3	0.5	0	0.3276(7)	0.0200(5)
Si1	0.2477(6)	0	0	0.0052(1)
Si2	0.2471(3)	2x	0	0.0052(1)
Al1	0.2504(7)	0	0.5	0.0052(1)
Al2	0.2506(4)	2x	0.5	0.0052(1)
O1	0.1117(2)	0.1990(4)	0.2415(1)	0.0107(1)
O2	0.0972(3)	0.6989(3)	0.2590(2)	0.0107(1)
O3	0.5971(3)	0.7048(3)	0.2643(2)	0.0107(1)
O4	0.6076(3)	0.2009(4)	0.2486(2)	0.0107(1)

* From Xu et al. (1999a).

† The temperature factors of like atoms and those for Al and Si are constrained to be equal.

eters for the ordered phases are plotted as $a'_o = a_o/2$, $c'_o = c_o/2$, and $V'_o = V_o/8$. The compositions were calculated from the starting stoichiometry. As shown in these figures, there are two transitions in the variation of a and c as a function of composition (x): with increasing silica content, a remains approximately unchanged from $x = 0$ to $x \sim 0.3$, and thereafter a decreases,

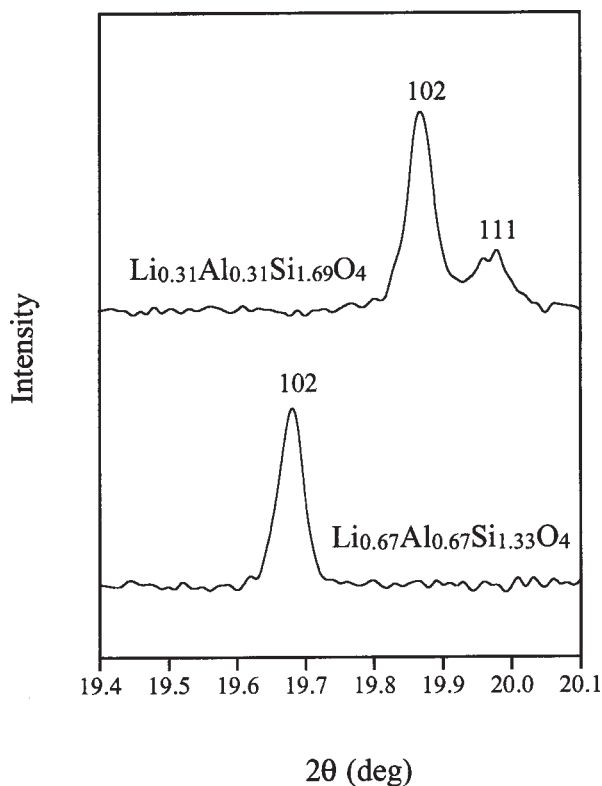


FIGURE 3. Synchrotron XRD patterns for the $\text{Li}_{1-x}\text{Al}_x\text{Si}_{1+x}\text{O}_4$ phases with (a) the stuffed β -quartz structure, $x = 0.33$ and (b) the stuffed α -quartz structure, $x = 0.69$. Note the 111 peak is evident in pattern (a) but not in (b).

TABLE 3. Atomic coordinates and isotropic temperature factors for the ordered stuffed β -quartz phase with a composition of $\text{Li}_{0.8}\text{Al}_{0.8}\text{Si}_{1.2}\text{O}_4$ (space group $F\bar{6}_222$)

Atom	x	y	z	U (\AA^2)*
Li1	0	0	0.5	0.025(6)
Li2	0.5	0	0	0.025(6)
Li3	0.5	0	0.316(4)	0.025(6)
(Si,Al)1	0.2504(8)	0	0	0.0079(3)
(Si,Al)2	0.2501(6)	2x	0	0.0079(3)
(Al,Si)1	0.2490(10)	0	0.5	0.0079(3)
(Al,Si)2	0.2503(6)	2x	0.5	0.0079(3)
O1	0.1078(14)	0.2061(13)	0.2438(8)	0.0134(9)
O2	0.0987(15)	0.6966(12)	0.2563(9)	0.0134(9)
O3	0.5913(10)	0.7010(11)	0.2779(6)	0.0134(9)
O4	0.5998(17)	0.2024(17)	0.2494(11)	0.0134(9)

* The temperature factors of like atoms and those for Al and Si are constrained to be equal.

with a change in slope at ~ 0.65 . In contrast, the cell parameter c exhibits a strong decrease between $x = 0$ and ~ 0.3 , remains roughly constant between $x \sim 0.3$ and ~ 0.65 , and decreases between $x \sim 0.65$ and 1. We interpret the two changes in trend at $x \sim 0.3$ and ~ 0.65 as consequences of two structural transformations across the series.

The lattice change at $x \sim 0.3$ corresponds to an Al-Si order-disorder transition as manifested by the disappearance of superlattice reflections for $x \geq \sim 0.3$. More specifically, the end-member β -eucryptite has a fully ordered Al-Si configuration, but as Si substitution for Li+Al increases, this order gradually decreases and disappears at ~ 0.3 . The change in slope at $x =$

~ 0.65 arises from the phase transition that is analogous to the β - α quartz transformation on cooling. As mentioned above, in the silica-rich phases with $x \geq \sim 0.65$, Li is not sufficiently abundant to prop open the β -quartz structure, so that the Al-Si framework collapses to the denser α -quartz modification. Because the changes in a and c near ~ 0.3 cancel, there is no significant discontinuity in the dependence of volume on Si substitution up to $x = \sim 0.65$, implying a continuous quality to the order-disorder transition. However, the displacive transition at $x = \sim 0.65$ occurs as a sharp change in slope due to the different densities of the α - and β -quartz frameworks.

Structural variations

The three compositional regimes delineated by the variations in cell parameters ($0 \leq x < \sim 0.3$, $\sim 0.3 \leq x < \sim 0.65$, and $\sim 0.65 \leq x \leq 1$) can be correlated to variations in crystal structure.

The $0 \leq x < \sim 0.3$ regime. Within this compositional range, the Al-Si distribution changes from the ordered state at $x = 0$ to the disordered configuration at $x = \sim 0.3$ (Figs. 4d, 4e). Lithium ions occupy only half of the available tetrahedral channel sites in end-member β -eucryptite (Tscherry et al. 1972b; Pillars and Peacor 1973; Xu et al. 1999a), but they tend to migrate to the other tetrahedral sites with increasing x (Nagel and Böhm 1982). When $x = \sim 0.3$, Li achieves complete positional disorder. As shown in Figure 4d, tetrahedral chains within the $[\text{SiO}_4]$ and $[\text{AlO}_4]$ sheets in ordered β -eucryptite are kinked, because individual tetrahedra distort to minimize Li-(Al, Si) repulsion and rotate away from the (001) plane (Xu et al. 1999a). By contrast, the Si(Al)-tetrahedral sheets in the disordered structure with $x \geq \sim 0.3$ are flat planar (Fig. 4e), as is reflected in the higher symmetry. The conversion from a puckered to a flat tetrahedral sheet involves the tilting of individual tetrahedra about the $\langle 100 \rangle$ axes. This “unpuckering” transformation may be envisioned as a stretching of the tetrahedral chains along $\langle 120 \rangle$. As a result, the overall structure expands along (001) but contracts parallel to c .

Because Si-tetrahedra are smaller than Al-tetrahedra (the mean $\langle \text{Al-O} \rangle$ bond distance is ~ 0.13 Å longer than $\langle \text{Si-O} \rangle$), the substitution of Si for Al can shorten the framework dimensions along both a and c . It appears that the net increase in a resulting from decreased tetrahedral distortion is canceled by the decrease due to Si substitution for Al, and thus a remains approximately constant for $0 \leq x < \sim 0.3$ (Fig. 5a). On the other hand, both tetrahedral tilting and Si substitution contribute to the framework contraction along the c -axis, thereby leading to a sharp drop in c between $x = 0$ and ~ 0.3 (Fig. 5b).

The $\sim 0.3 \leq x < \sim 0.65$ regime. Variations in cell parameters for $\sim 0.3 \leq x < \sim 0.65$ are opposite to those for $0 \leq x < \sim 0.3$. With increasing Si content, c remains nearly constant while a decreases (Figs. 5a and 5b). The trends exhibited by a and c for these compounds may be extrapolated to the pure silica end-member ($x = 1$), and these calculated values may be compared to hypothetical room-temperature cell parameters for pure β -quartz. Although pure β -quartz cannot exist metastably below 846 K, room-temperature unit-cell dimensions may be obtained by extrapolating β -quartz cell parameters measured at high-temperatures to 298 K (Carpenter et al. 1998a). As indicated in

Figure 5, the values extrapolated from the $\sim 0.3 \leq x < \sim 0.65$ regime match the hypothetical end-member parameters quite closely.

In the disordered, stuffed structure of β -quartz, Li shortens the O-O edges that are shared by the Li- and Si(Al)-tetrahedra to minimize Li-Si(Al) repulsion, which causes a contraction of the structure parallel to c and an expansion along a (Palmer 1994; Xu et al. 1999a). With increasing x , Li content decreases, and thus the effect of Li on cell dimensions becomes smaller. As a result, the cell parameter c tends to increase while a decreases with decreasing Li content. On the other hand, Si substitution for Al can shorten the cell dimensions along both c and a . Therefore, the preservation of the cell dimension c for $\sim 0.3 \leq x < \sim 0.65$ can be explained as a result of the counterbalance between a decrease arising from the Si \rightarrow Al substitution and an increase due to fewer Li ions within the channels. The reduced cell volume induced by substitution of Si for Al is reflected only in the a dimensions, and thereby the cell parameter a decreases with increasing x .

The $\sim 0.65 \leq x \leq 1$ regime. The phases within this compositional range adopt the denser α -quartz structure (Figs. 4c, 4f), and both a and c decrease with increasing x (Figs. 5a and 5b). The reduction in lattice parameters is caused by the substitution of Si for Al and the same kind of cooperative tetrahedral rotation that produces framework collapse in pure quartz with decreasing temperature. As shown in Figure 6a, the unit-cell volume decreases linearly with decreasing $\langle \text{T-O} \rangle$ bond distance, which in turn reflects the Si/Al ratio in the structure. The degree of rigid tetrahedral rotation around $\langle 100 \rangle$ can be described by the tilt angle δ :

$$\tan \delta = 2\sqrt{3}/9 (c/a) [(5 - 6z)/(1-x)],$$

TABLE 4. Atomic coordinates and isotropic temperature factors for the disordered $\text{Li}_{1-x}\text{Al}_{1-x}\text{Si}_{1+x}\text{O}_4$ phases*†

x	0.33	0.50‡	0.69	0.90‡
Space group	$F\bar{6}_222$	$F\bar{6}_222$	$P3_221$	$P3_221$
T(x)	0.5	0.5	0.5098(4)	0.5248(3)
T(y)	0	0	0	0
T(z)	0	0	2/3	2/3
O(x)	0.2053(2)	0.2052(2)	0.5883(3)	0.5887(5)
O(y)	2x	2x	0.7641(4)	0.7435(4)
O(z)	0.5	0.5	0.8110(4)	0.7940(4)
U(Li)§	0.013(4)	0.044(6)	0.063(15)	—
U(T)§	0.0117(3)	0.0169(2)	0.0132(2)	0.0131(3)
U(O)§	0.0223(6)	0.0312(6)	0.0218(7)	0.0200(7)

* The coordinates of Li for all compositions are 0, 0, 0.

† T = Si or Al.

‡ Only results for the major phase of the biphasic mixture are listed here.

§ In angstroms squared.

TABLE 5. T-O bond distances (in angstroms) for the $\text{Li}_{1-x}\text{Al}_{1-x}\text{Si}_{1+x}\text{O}_4$ phases*

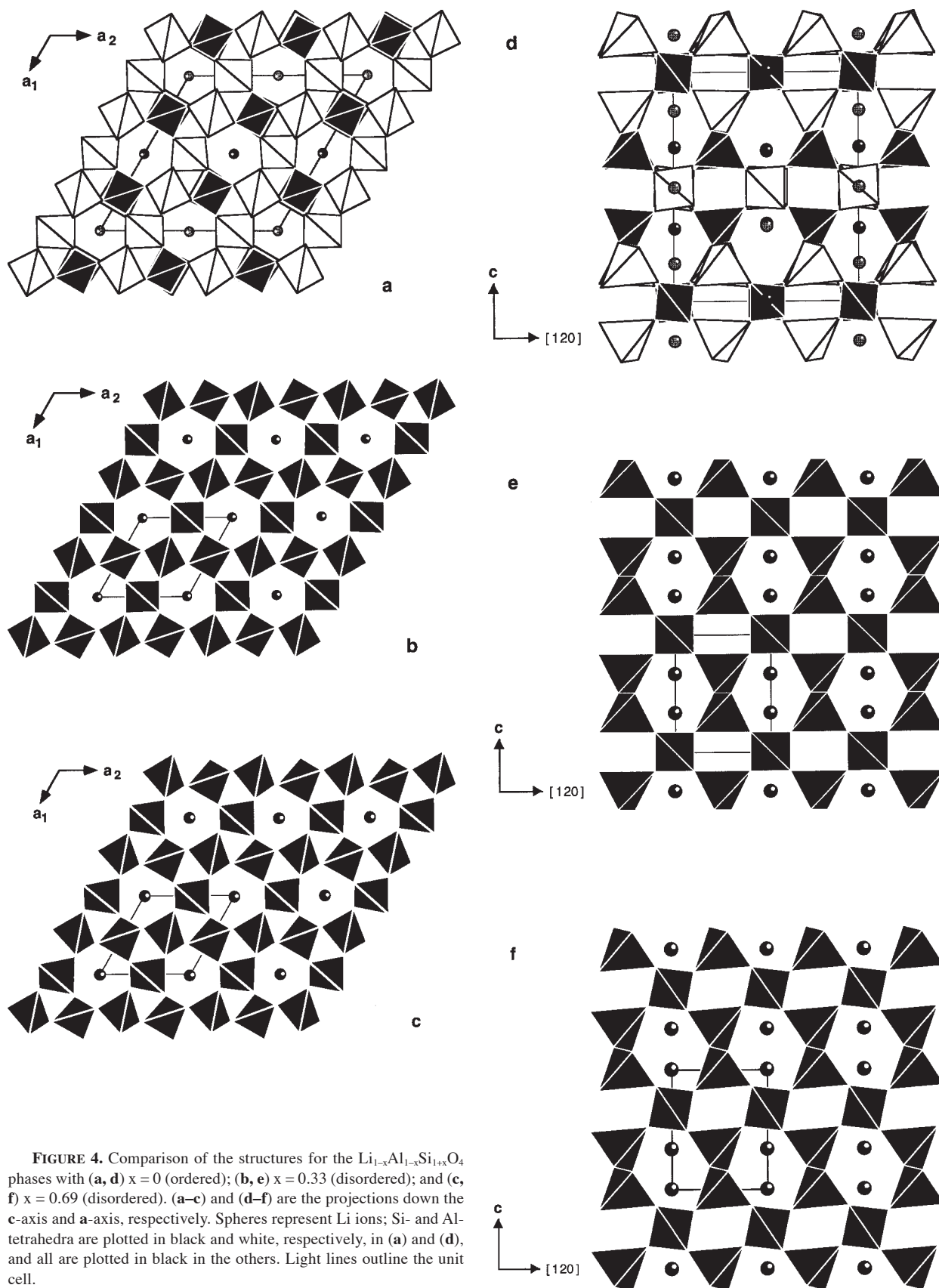
x	0	0.2	0.33	0.50§	0.69	0.90§
T-O1	1.631(2)†	1.64(1)‡	1.6388(4)	1.6295(4)	1.642(3)	1.614(3)
T-O2	1.721(3)†	1.70(1)‡	—	—	1.598(3)	1.609(3)

* T = Si or Al.

† T-O1 and T-O2 are averages of four Si-O and four Al-O bonds, respectively.

‡ T-O1 and T-O2 are averages of four (Si,Al)-O and four (Al,Si)-O bonds, respectively.

§ Only results for the major phase of the biphasic mixture are listed here.



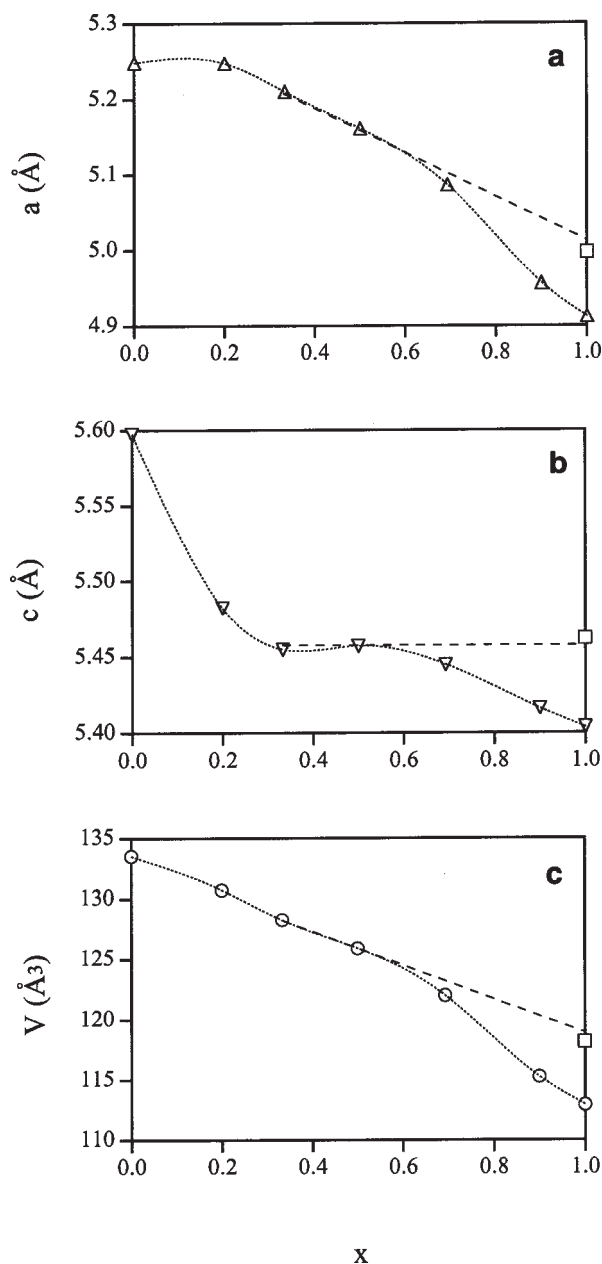


FIGURE 5. Variation of lattice parameters of the $\text{Li}_{1-x}\text{Al}_{1-x}\text{Si}_{1+x}\text{O}_4$ phases as a function of composition. (a) a -axis, (b) c -axis, and (c) cell volume V . Note the cell parameters for the ordered phases ($x=0$ and 0.2) are plotted as $a'_0 = a_0/2$, $c'_0 = c_0/2$, and $V'_0 = V_0/8$. The hypothetical room-temperature cell parameters of pure β -quartz are also shown for comparison (squares).

where a and c are lattice constants, and x and z are coordinates of oxygen (Grimm and Dörner 1975; Lager et al. 1982). Increasing the tilt angle δ decreases the cell volume (Fig. 6b). The steeper rate of decrease for a , c , and V with increasing x in the stuffed derivatives of α -quartz ($-0.65 \leq x \leq 1$) is due to this rigid tetrahedral rotation, which does not occur in the stuffed β -quartz structures (Fig. 5c).

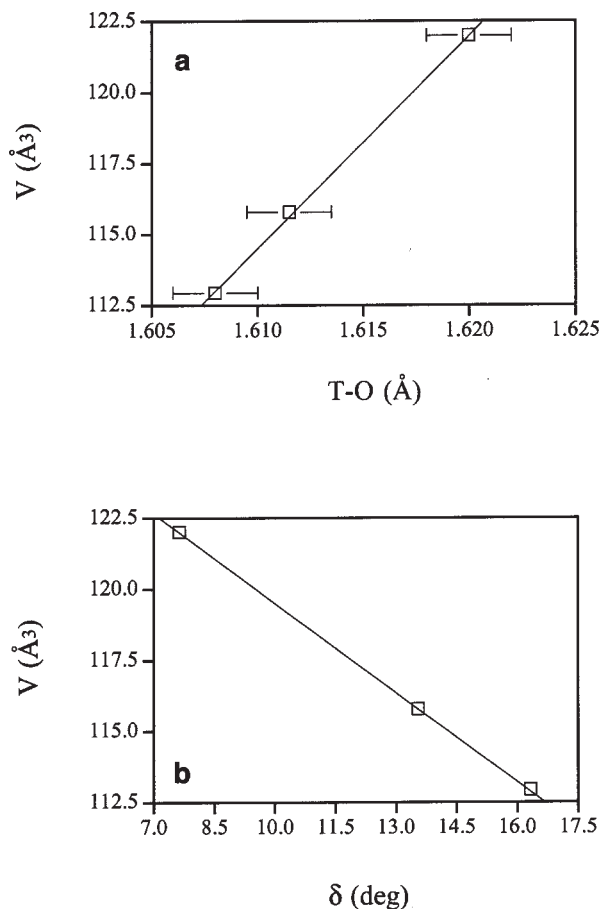


FIGURE 6. Variation in cell volume V for the stuffed α -quartz phases, $\text{Li}_{1-x}\text{Al}_{1-x}\text{Si}_{1+x}\text{O}_4$, as a function of the mean $\langle \text{T-O} \rangle$ bond length (a) and tilt angle δ (b). Data for the end-member α -quartz are from Will et al. (1988).

Spontaneous strain behavior at the α - β transition

Spontaneous strain has been used extensively to describe lattice distortions accompanying phase transitions that are induced by changing temperature (Salje 1990; Carpenter et al. 1998b). The similarities between the effects of Li+Al content and temperature on the quartz framework suggest that similar strain treatments can be used to characterize the α - β transition behavior using dopant content rather than temperature as the critical variable. Recently, Carpenter et al. (1998a) measured the temperature dependence of the spontaneous strains associated with the α - β quartz transition, and they documented the relationship between individual strains and the order parameter (Q) of the transition based on Landau theory.

Adopting the strain analysis method of Carpenter et al. (1998a) and using our own unit-cell parameter data for the stuffed derivatives of quartz with $\sim 0.3 \leq x \leq 1$ (Table 1; Fig. 5), we determined the spontaneous strains associated with the α - β transformation induced by the $\text{Li}^+ + \text{Al}^{3+} \rightarrow \text{Si}^{4+}$ substitution: $e_1 = e_2 = a/a_0 - 1$; $e_3 = c/c_0 - 1$, $V_s = V/V_0 - 1$, where e_1 , e_2 , and e_3 are the strain tensor components along the a -, b -, and c -axes, respectively; V_s is the volume strain; a , c , and V are parameters

of the stuffed derivatives of α -quartz; and a_0 , c_0 , and V_s are reference parameters determined from the variations in lattice dimensions of the β -quartz modifications within the LAS series.

As shown in Figure 7, the general strain behavior in stuffed derivatives of quartz as a function of Li+Al content [defined by $(1-x)$] closely parallels that observed in pure quartz as a function of temperature (Carpenter et al. 1998a). The magni-

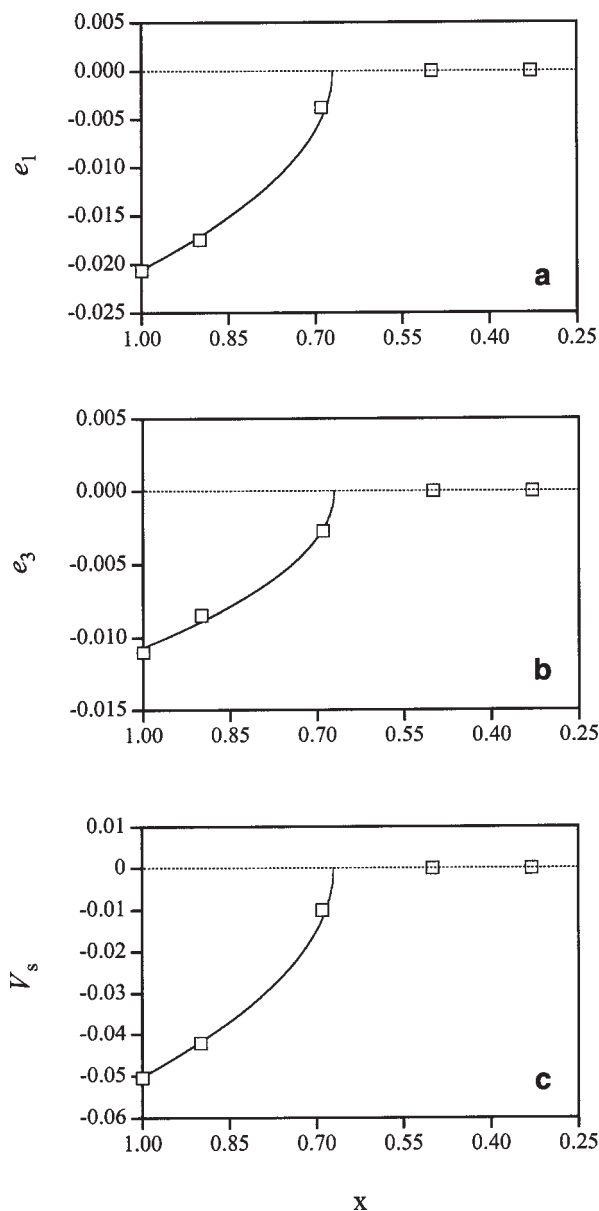


FIGURE 7. Variation of spontaneous strains for the $\text{Li}_{1-x}\text{Al}_{1-x}\text{Si}_{1+x}\text{O}_4$ phases as a function of composition. (a) e_1 , (b) e_3 , and (c) V_s . The curves are fits to the data with $x \geq x_c$ using the equation e_1 (or e_3 or V_s) = $A(x - x_c)^{1/2}$, where A is a constant, and x_c is the critical composition of the α - β transition, which was determined to be 0.67 from Figure 8. The values of A for e_1 , e_3 , and V_s are -0.0358 , -0.0186 , and -0.0873 , respectively. The dotted lines represent linear extrapolations of the data with $x < 0.67$ into the stability field for $x \geq 0.67$.

tudes of the spontaneous strains for the (Li+Al)-doped phases are of the same order as those for pure α -quartz ($T < T_c = 840$ K), although the former are somewhat smaller. For example, the values of e_1 , e_3 , and V_s for quartz at $T/T_c = 0.5$ are $\sim 1.5\%$, $\sim 0.9\%$, and $\sim 4\%$, respectively (Carpenter et al. 1998b), whereas the corresponding values for $\text{Li}_{1-x}\text{Al}_{1-x}\text{Si}_{1+x}\text{O}_4$ at $(1-x)/(1-x_c) = 0.5$ are $\sim 1.45\%$, $\sim 0.76\%$, and $\sim 3.54\%$.

The spontaneous strains that accompany a phase transition generally correlate with the order parameter Q by a coupling term in a Landau expansion of the Gibbs free energy (Salje 1990). Consequently, the evolution of spontaneous strains induced by temperature or composition can reveal the character of the transition. For the pure α - β quartz transformation, the strains can approximately be expressed as $e_1 \propto e_2 \propto V_s \propto Q^2$ (Carpenter et al. 1998a), and the temperature dependence of V_s^2 indicates that this transition is close to tricritical but is first order in nature. If the relation $e_1 \propto e_2 \propto V_s \propto Q^2$ also holds for the compositionally driven α - β transition in the $\text{Li}_{1-x}\text{Al}_{1-x}\text{Si}_{1+x}\text{O}_4$ system, the observed linear dependence of V_s^2 with x when $x > x_c$ (Fig. 8) suggests that this transition is close to tricritical as well. In addition, the good fits to the strain data in terms of the relation e_1 (or e_3 or V_s) = $A(x - x_c)^{1/2}$ (Fig. 7) are also consistent with the transition being close to tricritical in character. However, it is possible that a small jump in V_s^2 occurs near x_c , such that the compositionally driven transition has a small first-order character, like the thermally driven transition of the end-member. A conclusive determination of the nature of the transformation will require more strain data in the vicinity of the critical composition.

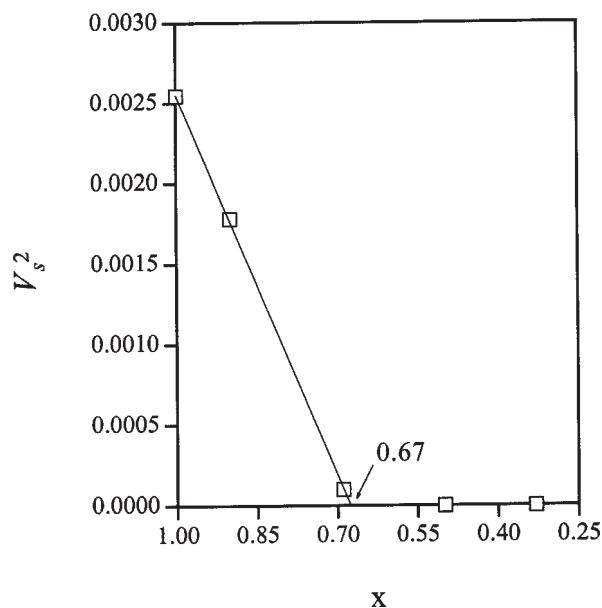


FIGURE 8. Variation of V_s^2 for the $\text{Li}_{1-x}\text{Al}_{1-x}\text{Si}_{1+x}\text{O}_4$ phases as a function of composition. Note that V_s^2 is linearly proportional to x when $x \geq x_c$.

ACKNOWLEDGMENTS

We are grateful to M.A. Carpenter, U. Bismayer, R.T. Downs, and J.E. Post for their constructive reviews of the manuscript and to D.E. Cox, P.M. Woodward, Q. Zhu, and D.M. Yates for assistance with synchrotron X-ray experiments. This work was supported by the NSF grants EAR-9418031 and EAR-9706143 (to P.J.H.) and the 1996 and 1997 ICDD crystallography scholarships (to H.X.). Synchrotron X-ray diffraction was carried out at the National Synchrotron Light Source (NSLS), Brookhaven National Laboratory, which is supported by the U.S. Department of Energy, Division of Material Sciences and Division of Chemical Sciences.

REFERENCES CITED

- Beall, G.H. (1994) Industrial applications of silica. In *Mineralogical Society of America Reviews in Mineralogy*, 29, 468–505.
- Buerger, M.J. (1954) The stuffed derivatives of the silica structures. *American Mineralogist*, 39, 600–614.
- Carpenter, M.A., Salje, E.K.H., Graeme-Barber, A., Wruck, B., Dove, M.T., and Knight, K.S. (1998a) Calibration of excess thermodynamic properties and elastic constant variations associated with the α - β phase transition in quartz. *American Mineralogist*, 83, 2–22.
- Carpenter, M.A., Salje, E.K.H., and Graeme-Barber, A. (1998b) Spontaneous strain as a determinant of thermodynamic properties for phase transitions in minerals. *European Journal of Mineralogy*, 10, 621–691.
- Cox, D.E., Toby, B.H., and Eddy, M.M. (1988) Acquisition of powder diffraction data with synchrotron radiation. *Australian Journal of Physics*, 41, 117–131.
- Dolino, G. and Vallade, M. (1994) Lattice dynamical behavior of anhydrous silica. In *Mineralogical Society of America Reviews in Mineralogy*, 29, 403–431.
- Dorogokupets, P.I. (1995) Equation of state for lambda transition in quartz. *Journal of Geophysical Research*, 100, 8489–8499.
- Finger, L.W., Cox, D.E., and Jephcoat, A.P. (1994) A correction for powder diffraction peak asymmetry due to axial divergence. *Journal of Applied Crystallography*, 27, 892–900.
- Ghiorso, M.S., Carmichael, I.S.E., and Moret, L.K. (1979) Inverted high-temperature quartz. *Contributions to Mineralogy and Petrology*, 68, 307–323.
- Grimm, H. and Dornier, B. (1975) On the mechanism of the α - β phase transformation of quartz. *Journal of Physics and Chemistry of Solids*, 36, 407–413.
- Guth, H. and Heger, G. (1979) Temperature dependence of the crystal structure of the one-dimensional Li⁺-conductor β -eucryptite (LiAlSiO₄). In P. Vashista, J.N. Mundy and G.K. Shenoy, Eds., *Fast ion transport in solids*, p. 499–502. Elsevier North Holland, New York.
- Hahn, T., Ed. (1996) *International Tables for Crystallography*, Volume A, Space-Group Symmetry, 878 p. Kluwer Academic Publishers, Dordrecht.
- Heaney, P.J. (1994) Structure and chemistry of the low-pressure silica polymorphs. In *Mineralogical Society of America Reviews in Mineralogy*, 29, 1–40.
- Heaney, P.J. and Veblen, D.R. (1991) Observation of the α - β transition in quartz: A review of imaging and diffraction studies and some new results. *American Mineralogist*, 76, 1018–1032.
- Keith, M.L. and Tuttle, O.F. (1952) Significance of variance in high-low inversion of quartz. *American Journal of Science*, 253a, 203–280.
- Lager, G.A., Jorgensen, J.D., and Rotella, F.J. (1982) Crystal structure and thermal expansion of α -quartz SiO₂ at low temperatures. *Journal of Applied Physics*, 53, 6751–6756.
- Lichtenstein, A.I., Jones, R.O., Xu, H., and Heaney, P.J. (1998) Anisotropic thermal expansion in the silicate β -eucryptite—A neutron diffraction and density functional study. *Physical Review B*, 58, 6219–6223.
- Larson, A.C. and Von Dreele, R.B. (1994) GSAS—General Structure Analysis System. Los Alamos National Laboratory Report No. LAUR 86–748, 179 p.
- Li, C.T. (1968) The crystal structure of LiAlSi₃O₈ III (high-quartz solid solution). *Zeitschrift für Kristallographie*, 127, 327–348.
- McGuinn, M.D. and Redfern, S.A.T. (1994) Ferroelastic phase transition along the join CaAl₂Si₂O₈-SrAl₂Si₂O₈. *American Mineralogist*, 79, 24–30.
- Müller, G. (1995) The scientific basis. In H. Bach, Ed., *Low thermal expansion glass ceramics*, p. 13–49. Springer-Verlag, Berlin.
- Nagel, W. and Böhm, H. (1982) Ionic conductivity studies on LiAlSiO₄-SiO₂ solid solutions of the high quartz type. *Solid State Communications*, 42, 625–631.
- Nakagawa, K. and Izumitani, T. (1972) Metastable phase separation and crystallization of Li₂O-Al₂O₃-SiO₂ glasses: Determination of miscibility gap from the lattice parameters of precipitated β -quartz solid solutions. *Journal of Non-Crystalline Solids*, 7, 168–180.
- O'Keefe, M. and Hyde, B.G. (1996) *Crystal structures. I. Patterns and symmetry*, 453 p. Mineralogical Society of America, Washington, D.C.
- Palmer, D.C. (1994) Stuffed derivatives of the silica polymorphs. In *Mineralogical Society of America Reviews in Mineralogy*, 29, 83–122.
- Petzoldt, J. (1967) Metastabile mischkristalle mit quarzstruktur mit oxidsystem Li₂O-MgO-ZnO-Al₂O₃-SiO₂. *Glastechnische Berichte*, 40, 385–396.
- Phillips, B.L., Xu, H., Heaney, P.J., and Navrotsky, A. (2000) ²⁹Si and ²⁷Al MAS-NMR spectroscopy of β -eucryptite (LiAlSiO₄): the enthalpy of Si,Al ordering. *American Mineralogist*, 85, 181–188.
- Pillars, W.W. and Peacor, D.R. (1973) The crystal structure of beta eucryptite as a function of temperature. *American Mineralogist*, 58, 681–690.
- Ribbe, P.H. (1983) Aluminum-silicon order in feldspars: Domain textures and diffraction patterns. In *Mineralogical Society of America Reviews in Mineralogy*, 2, 21–55.
- Roy, R. (1995) Low thermal expansion ceramics: A retrospective. In: Stinton and Limaye (eds.), *Low-expansion materials*, Ceramic Transactions, Vol. 52, The American Ceramic Society, 1–4.
- Salje, E.K.H. (1990) Phase transitions in ferroelastic and co-elastic crystals, 366 p. Cambridge University Press, Cambridge.
- Salje, E.K.H., Bismayer, U., Wruck, B., and Hensler, J. (1991) Influence of lattice imperfections on the transition temperatures of structural phase transitions: The plateau effect. *Phase Transitions*, 35, 61–70.
- Schulz, H. (1974) Thermal expansion of beta eucryptite. *Journal of the American Ceramic Society*, 57, 313–317.
- Schulz, H. and Tscherry, V. (1972a) Structural relations between the low- and high-temperature forms of β -eucryptite (LiAlSiO₄) and low and high quartz. I. Low-temperature form of β -eucryptite and low quartz. *Acta Crystallographica*, B28, 2168–2173.
- (1972b) Structural relations between the low- and high-temperature forms of β -eucryptite (LiAlSiO₄) and low and high quartz. II. High-temperature form of β -eucryptite and high quartz. *Acta Crystallographica*, B28, 2174–2177.
- Smith, J.V. and Steele, I.M. (1984) Chemical substitution in silica polymorphs. *Neues Jahrbuch für Mineralogie. Monatshefte*, 3, 137–144.
- Thompson, P., Cox, D.E., and Hastings, J. (1987) Rietveld refinement of Debye-Scherrer synchrotron X-ray data for Al₂O₃. *Journal of Applied Crystallography*, 20, 79–83.
- Tscherry, V. and Laves, F. (1970) Synthesis and x-ray reflection pattern of β -eucryptite. *Naturwissenschaften*, 57, 194.
- Tscherry, V., Schulz, H., and Laves, F. (1972a) Average and super structure of β -eucryptite (LiAlSiO₄), Part I, Average structure. *Zeitschrift für Kristallographie*, 135, 161–174.
- (1972b) Average and super structure of β -eucryptite (LiAlSiO₄), Part II, Superstructure. *Zeitschrift für Kristallographie*, 135, 175–198.
- Will, G., Bellotto, M., Parrish, W., and Hart, M. (1988) Crystal structures of quartz and magnesium germanate by profile analysis of powder diffractometer data. *Journal of Applied Crystallography*, 21, 182–191.
- Winkler, H.G.F. (1948) Synthese und Kristallstruktur des Eukryptits, LiAlSiO₄. *Acta Crystallographica*, 1, 27–34.
- Xu, H., Heaney, P.J., Yates, D.M., Von Dreele, R.B., and Bourke, M.A. (1999a) Structural mechanisms underlying near-zero thermal expansion in β -eucryptite: A combined synchrotron X-ray and neutron Rietveld analysis. *Journal of Materials Research*, 14, 3138–3151.
- Xu, H., Heaney, P.J., Navrotsky, A., Topor, L., and Liu, J. (1999b) Thermochemistry of stuffed quartz-derivative phases along the join LiAlSiO₄-SiO₂. *American Mineralogist*, 84, 1360–1369.
- Xu, H., Heaney, P.J., and Böhm, H. (1999c) Structural modulations and phase transitions in β -eucryptite: An in-situ TEM study. *Physics and Chemistry of Minerals*, 26, 633–643.

MANUSCRIPT RECEIVED SEPTEMBER 9, 1999

MANUSCRIPT ACCEPTED JANUARY 31, 2000

PAPER HANDLED BY JEFFREY E. POST